

On the topological entropy of (a, b) -continued fraction transformations

Adam Abrams¹ , Svetlana Katok² and Ilie Ugarcovici^{3,*} 

¹ Faculty of Pure and Applied Mathematics, Wrocław University of Science and Technology, Wrocław 50370, Poland

² Department of Mathematics, The Pennsylvania State University, University Park, PA 16802, United States of America

³ Department of Mathematical Sciences, DePaul University, Chicago, IL 60614, United States of America

E-mail: iugarcov@depaul.edu

Received 20 October 2022; revised 18 March 2023

Accepted for publication 22 March 2023

Published 12 April 2023

Recommended by Dr Vaughn Climenhaga



Abstract

We study the topological entropy of a two-parameter family of maps related to (a, b) -continued fraction algorithms and prove that it is constant on a square within the parameter space (two vertices of this square correspond to well-studied continued fraction algorithms). The proof uses conjugation to maps of constant slope. We also present experimental evidence that the topological entropy is flexible (i.e. takes any value in a range) on the whole parameter space.

Keywords: continued fraction maps, one-dimensional dynamics, topological entropy, Markov partitions

Mathematics Subject Classification numbers: 37E05, 37B40

(Some figures may appear in colour only in the online journal)

1. Introduction

The dynamics of piecewise monotone interval maps, and in particular their topological entropy and conjugation to maps of constant slope, has been a rich area of investigation, going back to fundamental work of Parry [24]. See also the monographs [4, 11] and references therein. Within this class of interval maps, a considerable amount of work has been done for unimodal

* Author to whom any correspondence should be addressed.

maps. Boundary maps associated to co-compact Fuchsian groups (see [1]) provide an important family of piecewise monotone examples with multiple discontinuity points. In this paper, we study the topological entropy of a two-parameter family of boundary maps $f_{a,b} : \mathbb{R} \rightarrow \mathbb{R}$, where $\mathbb{R} = \mathbb{R} \cup \{\infty\}$, associated to the (not co-compact) modular group $\text{PSL}(2, \mathbb{Z})$. These transformations were introduced in [17] and are given by

$$f_{a,b}(x) := \begin{cases} x + 1 & \text{if } x < a \\ -\frac{1}{x} & \text{if } a \leq x < b \\ x - 1 & \text{if } x \geq b, \end{cases} \tag{1}$$

where the parameters a, b belong to the set

$$\mathcal{P} := \{(a, b) \in \mathbb{R}^2 \mid a \leq 0 \leq b, b - a \geq 1, -ab \leq 1\}.$$

Although we do not focus on number-theoretic applications in this paper, the maps $f_{a,b}$ can be used to construct continued fraction expansions: for any $x \in \mathbb{R}$,

$$x = n_0 - \frac{1}{n_1 - \frac{1}{n_2 - \frac{1}{n_3 - \dots}}} := [n_0, n_1, n_2, \dots]_{a,b},$$

where $|n_k|$ is the number of iterates under $f_{a,b}$ in between successive visits to $[a, b]$, and the sign of n_k shows whether the iterates are to the left or right of $[a, b]$. This is explained in more detail, with the same notations, in [17, section 2]. We refer to $f_{a,b}$ as a ‘slow’ continued fraction map, in contrast to a Gauss-like map (the first return of $f_{a,b}$ to the interval $[a, b]$). Several particular parameter choices correspond to well-studied continued fraction algorithms (see [16, 17] for references): the case $(a, b) = (-1, 1)$ corresponds to regular (plus) continued fractions with alternating signs for digits (it is also related to a method of symbolically coding the geodesic flow on the modular surface following Artin’s pioneering work), and the case $(a, b) = (-\frac{1}{2}, \frac{1}{2})$ gives the ‘nearest-integer’ continued fractions considered first by Hurwitz. These two cases play a pivotal role in section 2.2. The case $(a, b) = (-1, 0)$ is also noteworthy, corresponding to the classical minus (also called backwards) continued fractions; this case will be mentioned again in section 3.

The notion of topological entropy was introduced by Adler, Konheim, and McAndrew in [3]. Their definition used covers and applied to compact Hausdorff spaces; Dinaburg [12] and Bowen [7] gave definitions involving distance functions and separated sets, which are often more suitable for calculation. While these formulations of topological entropy were originally intended for continuous maps acting on compact spaces, Bowen’s definition can actually be applied to piecewise continuous, piecewise monotone maps on an interval, as explained in [22]. The most convenient definition of topological entropy for piecewise continuous piecewise monotone maps is

$$h_{\text{top}}(f) = \lim_{n \rightarrow \infty} \frac{\log(\#\text{of laps of } f^n)}{n},$$

where a *lap* is a maximal interval of monotonicity for a function [4, 21]. In [22] it is shown that this agrees with Bowen’s definition of topological entropy. When a map is *Markov*, i.e. it admits a finite Markov partition (see [14, chapter 1.9]), its topological entropy can be found explicitly as the log of the spectral radius (the maximum absolute value of the eigenvalues) of the associated transition matrix.

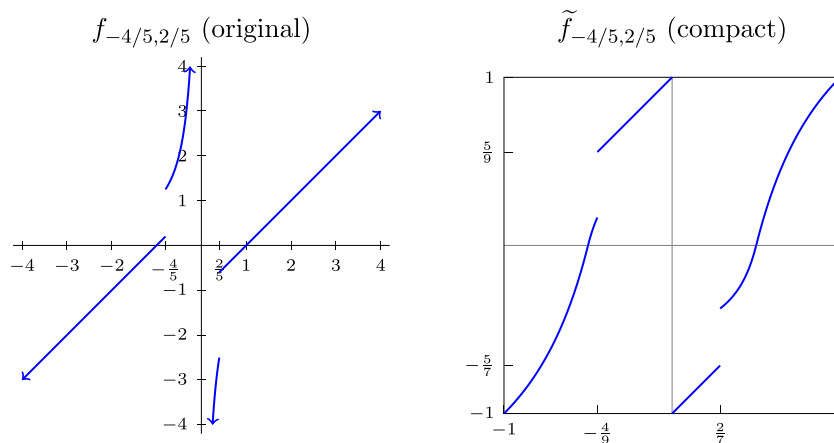


Figure 1. Plots of $f_{a,b}$ and $\tilde{f}_{a,b}$ for $a = -\frac{4}{5}, b = \frac{2}{5}$.

As a one-dimensional map on $\overline{\mathbb{R}}$, each $f_{a,b}$ is piecewise continuous and piecewise monotone. The map

$$k(x) := \frac{x}{1 + |x|}$$

is a homeomorphism from $\overline{\mathbb{R}}$ to $[-1, 1]/\sim$ with ± 1 identified; for convenience, we will write only $[-1, 1]$ and deal with interval maps, although the results and proofs could all be done on a circle. To make our notation more uniform, we conjugate the standard generators

$$T(x) := x + 1 \quad \text{and} \quad S(x) := -\frac{1}{x}$$

of the modular group $PSL(2, \mathbb{Z})$ to

$$\tilde{T} := k \circ T \circ k^{-1} \quad \text{and} \quad \tilde{S} := k \circ S \circ k^{-1}$$

(see figure 6 on page 6) and conjugate our continued fraction map $f_{a,b} : \overline{\mathbb{R}} \rightarrow \overline{\mathbb{R}}$ to the map $\tilde{f}_{a,b} : [-1, 1] \rightarrow [-1, 1]$,

$$\tilde{f}_{a,b}(x) := k \circ f_{a,b} \circ k^{-1}(x) = \begin{cases} \tilde{T}(x) & \text{if } -1 \leq x < \frac{a}{1-a} \\ \tilde{S}(x) & \text{if } \frac{a}{1-a} \leq x < \frac{b}{1+b} \\ \tilde{T}^{-1}(x) & \text{if } \frac{b}{1+b} \leq x \leq 1, \end{cases} \quad (2)$$

thus obtaining a piecewise monotone map with two discontinuity points $k(a)$ and $k(b)$, see figure 1 (note that on the right, $k(a) = -\frac{4}{9}$ and $k(b) = \frac{2}{7}$).

In this paper, we prove the following ‘entropy plateau’ result:

Theorem 1. For any $(a, b) \in \mathcal{S} = [-1, -\frac{1}{2}] \times [\frac{1}{2}, 1] \subset \mathcal{P}$, the topological entropy of $\tilde{f}_{a,b}$ (and, therefore, of $f_{a,b}$) is $\log(\frac{1+\sqrt{5}}{2})$.

The ‘golden square’ $\mathcal{S} = [-1, -\frac{1}{2}] \times [\frac{1}{2}, 1] \subset \mathcal{P}$ is highlighted in figure 2. Note that this subset contains (uncountably many) parameters for which $\tilde{f}_{a,b}$ does not admit a Markov partition, and our entropy formula holds for these maps as well. Also note that maps from this family are not necessarily topologically conjugate to each other because the combinatorial structure of the orbits of the discontinuity points can differ (see [17, section 4]).

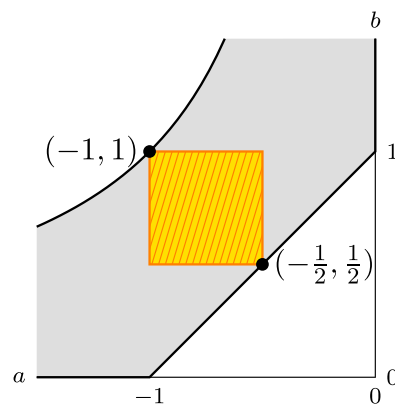


Figure 2. The parameter space \mathcal{P} , with the ‘golden square’ \mathcal{S} shaded.

Remark 2. For a special family of piecewise affine maps with one discontinuity point, an entropy plateau phenomenon was investigated by Bruin, Carminati, Marmi, and Profeti [9] and by Cosper and Misiurewicz [10] (they call it ‘entropy locking’). Both papers follow numerical simulations from Botella-Soler *et al* [6]. Our maps $f_{a,b}$ are piecewise monotone and have two discontinuity points, so their methods do not readily apply here.

Remark 3. In [18, sections 6 and 7], the authors obtained an absolutely continuous invariant probability measure for the first return (Gauss-like) map of $f_{a,b}$ to $[a, b)$. With respect to this measure, the entropy of the Gauss-like map is $\frac{1}{K_{a,b}} \frac{\pi^2}{3}$ [18, theorem 6.2], where $K_{a,b}$ is the measure of the domain of the natural extension (which is finite). By lifting this measure to \mathbb{R} , one obtains an infinite invariant measure for $f_{a,b} : \mathbb{R} \rightarrow \mathbb{R}$, so the classical notion of measure-theoretic entropy does not apply to $f_{a,b}$. It is an almost immediate consequence of [18, theorem 6.2] that the ‘Krengel entropy’ (see [20]) of $f_{a,b}$ is $\frac{\pi^2}{3}$ for all $(a, b) \in \mathcal{P}$.

2. Proof of main result

The proof of theorem 1 uses results about conjugacy to piecewise continuous maps with constant slope (see [5]). Specifically, we prove that the maps $\tilde{f}_{-1,1}$ and $\tilde{f}_{-1/2,1/2}$ are conjugate to piecewise linear maps with constant slope $\frac{1+\sqrt{5}}{2}$ using *the same conjugacy*. We then show that this conjugacy will also conjugate any $\tilde{f}_{a,b}$ with $(a, b) \in [-1, -\frac{1}{2}] \times [\frac{1}{2}, 1]$ to a map with constant slope $\frac{1+\sqrt{5}}{2}$. A similar argument was first used by the authors in [1] for maps related to co-compact Fuchsian groups. An important ingredient of this approach is a symbolic ‘recoding’ process, addressed in lemma 7 below. The recoding in this paper turns out to be less intricate than the corresponding recoding in [1, appendix A].

2.1. Conjugation to maps of constant slope

In [24], following his seminal work [23], Parry proved that a continuous, piecewise monotone, strongly transitive interval map with positive topological entropy is conjugate to a constant slope map. In [5], following [4], Alsedà and Misiurewicz generalized this to a semi-conjugacy result for piecewise continuous, piecewise monotone interval maps that are not necessarily transitive. For the present paper, we need only the original results of Parry.

Theorem 4 ([24, theorem 5]). *Let I be a compact interval and let $g : I \rightarrow I$ be a piecewise continuous, piecewise monotone, strongly⁴ transitive map with positive topological entropy $h > 0$. There exists an increasing homeomorphism $\psi : I \rightarrow I$ conjugating g to a piecewise continuous map with constant slope e^h .*

In the case where $\tilde{f}_{a,b}$ is Markov, the conjugacy $\psi_{a,b}$ can be obtained by the classical construction due to Parry [24] and used in the proof of [5, lemma 5.1]. We define the probability measure $\rho_{a,b}$ on the shift space $X_{a,b} \subset \{1, \dots, N\}^{\mathbb{N}}$ as follows: let λ, ν (possibly depending on a, b) be the maximal eigenpair for the Markov transition matrix $M_{a,b}$; for an (a, b) -admissible finite sequence $(\omega_0, \dots, \omega_n)$ (that is, for which $(M_{a,b})_{\omega_i, \omega_{i+1}} = 1$ for $i = 0, \dots, n - 1$), we denote a symbolic cylinder of rank $n + 1$ as

$$C_{a,b}(\omega_0, \dots, \omega_n) := \{ \omega' \in X_{a,b} \mid \omega'_i = \omega_i \ \forall 0 \leq i \leq n \}$$

and define the measure $\rho_{a,b}$ of this cylinder to be

$$\rho_{a,b}(C_{a,b}(\omega_0, \dots, \omega_n)) = \frac{\nu_{\omega_n}}{\lambda^n}. \tag{3}$$

The measure $\rho_{a,b}$ is equivalent to the shift-invariant ‘Parry measure’ (the measure of maximal entropy; see [23, 24]). The measure $\rho_{a,b}$ is not shift-invariant but has the ‘expanding property’

$$\rho_{a,b}(\sigma_{a,b}(C)) = \lambda \cdot \rho_{a,b}(C)$$

for all cylinders C on $(X_{a,b}, \sigma_{a,b})$.

Using the measure $\rho_{a,b}$, one constructs the push-forward Borel probability measure $\rho'_{a,b}$ on $[-1, 1]$ given by

$$\rho'_{a,b}(E) = \rho_{a,b}(\phi_{a,b}^{-1}(E)) \quad \text{for Borel } E \subset [-1, 1],$$

where $\phi_{a,b} : X_{a,b} \rightarrow [-1, 1]$ is the (essentially bijective) symbolic coding map, that is, $\phi_{a,b}(\omega) = \bigcap_{i=0}^{\infty} \tilde{f}_{a,b}^{-i}(I_{\omega_i})$. The conjugacy $\psi_{a,b} : [-1, 1] \rightarrow [-1, 1]$ is given by

$$\psi_{a,b}(x) := -1 + 2 \cdot \rho'_{a,b}([-1, x]). \tag{4}$$

The presence of -1 and 2 in the formula (4) comes from our use of $[-1, 1]$ as the domain for $\tilde{f}_{a,b}$.

2.2. Artin and Hurwitz parameters

We consider two particular parameter choices: the ‘Artin’ case $(a, b) = (-1, 1)$ and the ‘Hurwitz’ case $(a, b) = (-\frac{1}{2}, \frac{1}{2})$. From now on, we abbreviate $\tilde{f}_A = \tilde{f}_{-1,1}$, $\psi_A = \psi_{-1,1}$, etc and $\tilde{f}_H = \tilde{f}_{-1/2,1/2}$, $\psi_H = \psi_{-1/2,1/2}$, etc.

The maps \tilde{f}_A and \tilde{f}_H are each piecewise monotone, piecewise continuous, and Markov with respect to the same partition $\{I_1, \dots, I_8\}$ of the interval $[-1, 1]$ (see figure 3):

$$\begin{aligned} I_1 &= [-1, -\frac{2}{3}], & I_2 &= [-\frac{2}{3}, -\frac{1}{2}], & I_3 &= [-\frac{1}{2}, -\frac{1}{3}], & I_4 &= [-\frac{1}{3}, 0], \\ I_5 &= [0, \frac{1}{3}], & I_6 &= [\frac{1}{3}, \frac{1}{2}], & I_7 &= [\frac{1}{2}, \frac{2}{3}], & I_8 &= [\frac{2}{3}, 1]. \end{aligned}$$

The associated Markov diagrams are shown in figure 4.

⁴ A map $f : X \rightarrow X$ is *strongly transitive* if for any nonempty open set $U \subset X$ there exists n such that $\bigcup_{i=1}^n f^i(U) = X$. For piecewise monotone interval maps, transitivity implies strong transitivity [13].

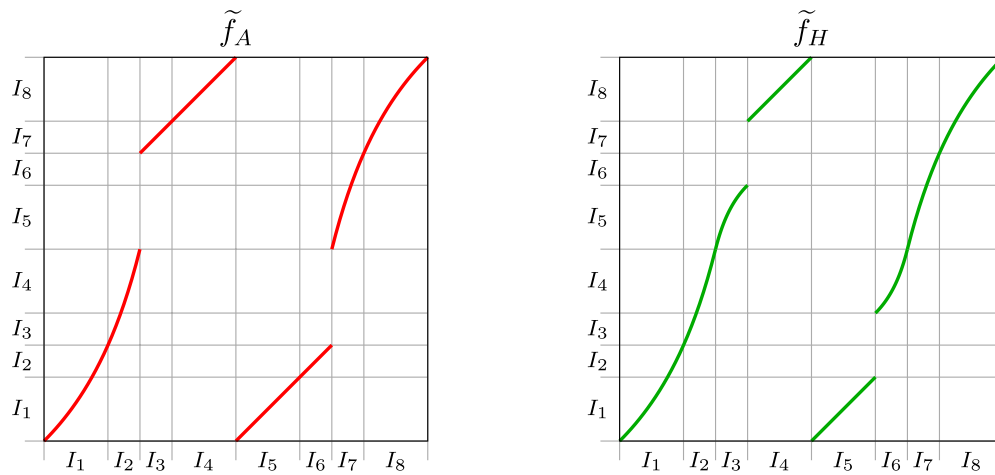


Figure 3. Plots of $\tilde{f}_A = \tilde{f}_{-1,1}$ and $\tilde{f}_H = \tilde{f}_{-1/2,1/2}$ with their (shared) Markov partition of $[-1, 1]$.

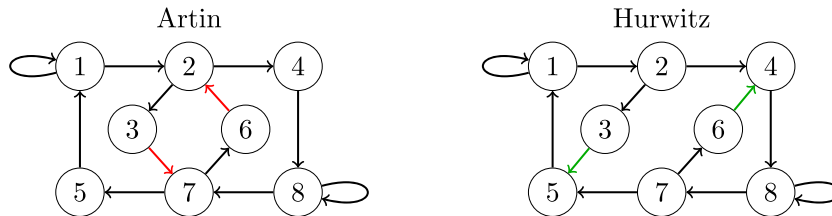


Figure 4. Markov structure of Artin and Hurwitz admissibility.

From the Markov diagrams, we construct the pair of 8×8 transition matrices

$$M_A = \begin{pmatrix} 1 & 1 & 0 & 0 & 0 & 0 & 0 & 0 \\ 0 & 0 & 1 & 1 & 0 & 0 & 0 & 0 \\ 0 & 0 & 0 & 0 & 0 & 0 & 1 & 0 \\ 0 & 0 & 0 & 0 & 0 & 0 & 0 & 1 \\ 1 & 0 & 0 & 0 & 0 & 0 & 0 & 0 \\ 0 & 1 & 0 & 0 & 0 & 0 & 0 & 0 \\ 0 & 0 & 0 & 0 & 1 & 1 & 0 & 0 \\ 0 & 0 & 0 & 0 & 0 & 0 & 1 & 1 \end{pmatrix}, \quad M_H = \begin{pmatrix} 1 & 1 & 0 & 0 & 0 & 0 & 0 & 0 \\ 0 & 0 & 1 & 1 & 0 & 0 & 0 & 0 \\ 0 & 0 & 0 & 0 & 1 & 0 & 0 & 0 \\ 0 & 0 & 0 & 0 & 0 & 0 & 0 & 1 \\ 1 & 0 & 0 & 0 & 0 & 0 & 0 & 0 \\ 0 & 0 & 0 & 1 & 0 & 0 & 0 & 0 \\ 0 & 0 & 0 & 0 & 1 & 1 & 0 & 0 \\ 0 & 0 & 0 & 0 & 0 & 0 & 1 & 1 \end{pmatrix}. \quad (5)$$

Notice that the two matrices are very similar, the only difference being that the transitions $I_3 \rightarrow I_7$ and $I_6 \rightarrow I_2$ in M_A are replaced by $I_3 \rightarrow I_5$ and $I_6 \rightarrow I_4$ in M_H .

Using these matrices, we can now prove that \tilde{f}_A and \tilde{f}_H satisfy the transitivity condition of theorem 4: by [14, proposition 1.9.9] a Markov shift is transitive (in fact, topologically mixing) if some finite power of its transition matrix has all positive values, and indeed M_A^6 and M_H^6 have all positive values.

By direct computation, the characteristic polynomials of M_A and M_H are

$$(x^2 - x - 1)(x^2 - x + 1)x^4 \quad \text{and} \quad (x^2 - x - 1)(x^2 - x + 1)(x^4 - 1),$$

respectively, and so both have the same dominant eigenvalue

$$\lambda = \frac{1 + \sqrt{5}}{2}.$$

The corresponding (right probability) eigenvector for both matrices is

$$v = \frac{1}{6\lambda + 4}(\lambda + 1, \lambda, 1, \lambda, \lambda, 1, \lambda, \lambda + 1). \tag{6}$$

To aid in later proofs, we denote $A_k = \tilde{f}_A|_{I_k}$ and $H_k = \tilde{f}_H|_{I_k}$. The following lemma can be proven by looking at the graphs in figure 3 or by a careful analysis of (2) on the intervals I_1, \dots, I_8 :

Lemma 5. *The maps A_1, A_2, H_1, H_2, H_3 coincide with \tilde{T} . The maps $A_3, A_4, A_5, A_6, H_4, H_5$ coincide with \tilde{S} . The maps A_7, A_8, H_6, H_7, H_8 coincide with \tilde{T}^{-1} . In particular, if $k \notin \{3, 6\}$, then $A_k = H_k$.*

By theorem 4 there exists a (unique) increasing homeomorphism $\psi_A : [-1, 1] \rightarrow [-1, 1]$ conjugating \tilde{f}_A to a map

$$\ell_A := \psi_A \circ \tilde{f}_A \circ \psi_A^{-1}$$

with constant slope $\lambda = \frac{1 + \sqrt{5}}{2}$, and there exists a (unique) increasing homeomorphism $\psi_H : [-1, 1] \rightarrow [-1, 1]$ conjugating \tilde{f}_H to a map

$$\ell_H := \psi_H \circ \tilde{f}_H \circ \psi_H^{-1}$$

also with constant slope $\frac{1 + \sqrt{5}}{2}$.

We will prove that the maps ψ_A and ψ_H (each obtained by Parry’s construction) coincide:

Theorem 6. *For all $x \in [-1, 1]$, $\psi_A(x) = \psi_H(x)$.*

Equivalently, $\rho'_A(J) = \rho'_H(J)$ for all intervals $J \subset [-1, 1]$. It is sufficient to take J to be a cylinder interval: given an (a, b) -admissible sequence $\omega = (\omega_0, \omega_1, \dots, \omega_n)$ with $\omega_i \in \{1, \dots, 8\}$, we define the corresponding (a, b) -cylinder interval of rank $n + 1$ as

$$\begin{aligned} I_{a,b}(\omega_0, \omega_1, \dots, \omega_n) &:= I_{\omega_0} \cap \tilde{f}_{a,b}^{-1}(I_{\omega_1}) \cap \dots \cap \tilde{f}_{a,b}^{-n}(I_{\omega_n}) \\ &= I_{\omega_0} \cap \tilde{f}_{a,b}^{-1}(I_{a,b}(\omega_1, \dots, \omega_n)). \end{aligned} \tag{7}$$

If every A -admissible word $\omega = (\omega_0, \dots, \omega_n)$ had a corresponding H -admissible $\tau = (\tau_0, \dots, \tau_n)$ with $I_A(\omega) = I_H(\tau)$ and $v_{\omega_n} = v_{\tau_n}$ then theorem 6 would be proven. In fact, we do not need to show $I_A(\omega) = I_H(\tau)$ for all A -admissible ω , as we now explain.

If $\omega_n \in \{3, 4, 5, 6\}$, then we use the unique Markov transitions $3 \rightarrow 7, 4 \rightarrow 8, 5 \rightarrow 1$ and $6 \rightarrow 2$ to instead consider

$$\begin{aligned} I_A(\omega_0, \dots, \omega_{n-1}, 3) &= I_A(\omega_0, \dots, \omega_{n-1}, 3, 7), \\ I_A(\omega_0, \dots, \omega_{n-1}, 4) &= I_A(\omega_0, \dots, \omega_{n-1}, 4, 8), \\ I_A(\omega_0, \dots, \omega_{n-1}, 5) &= I_A(\omega_0, \dots, \omega_{n-1}, 5, 1), \\ I_A(\omega_0, \dots, \omega_{n-1}, 6) &= I_A(\omega_0, \dots, \omega_{n-1}, 6, 2). \end{aligned}$$

Therefore we can assume $\omega_n \notin \{3, 4, 5, 6\}$.

Lemma 7. *If $\omega = (\omega_0, \dots, \omega_n)$ is A -admissible and $\omega_n \in \{1, 2, 7, 8\}$, then there exists an H -admissible word $\tau = (\tau_0, \dots, \tau_n)$ such that $\omega_0 = \tau_0$ and $I_A(\omega) = I_H(\tau)$. Moreover, if $\omega_n \in \{1, 8\}$, then $\omega_n = \tau_n$; if $\omega_n = 2$, then $\tau_n \in \{2, 4\}$; and if $\omega_n = 7$, then $\tau_n \in \{5, 7\}$.*

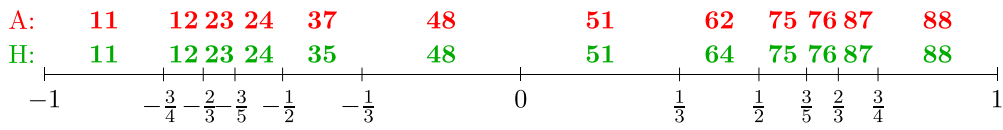


Figure 5. Rank-two cylinder intervals for \tilde{f}_A (top) and \tilde{f}_H (bottom) coincide.

Proof. Recall the notation A_k and H_k from lemma 5. From the monotonicity of A_k and H_k , we can avoid the intersection in the definition (7) and instead calculate

$$I_A(\omega_0, \omega_1, \dots, \omega_n) = A_{\omega_0}^{-1}(I_A(\omega_1, \dots, \omega_n)) \quad \text{if } (\omega_0, \omega_1, \dots, \omega_n) \text{ is } A\text{-admissible}$$

and

$$I_H(\tau_0, \tau_1, \dots, \tau_n) = H_{\tau_0}^{-1}(I_H(\tau_1, \dots, \tau_n)) \quad \text{if } (\tau_0, \tau_1, \dots, \tau_n) \text{ is } H\text{-admissible.}$$

With these observations, in figure 5 we have the following correspondence between the rank two cylinder intervals of the two maps.

The matching $I_A(1, 1) = I_H(1, 1)$ and $I_A(1, 2) = I_H(1, 2)$ and similarly for $(2, 3)$, $(2, 4)$, $(4, 8)$, $(5, 1)$, $(7, 5)$, $(7, 6)$, $(8, 7)$, and $(8, 8)$ are all trivial due to lemma 5. One can also check directly that

$$I_A(3, 7) = I_H(3, 5) = I_3 \quad \text{and} \quad I_A(6, 2) = I_H(6, 4) = I_6.$$

We have the following identities:

$$\begin{aligned} I_A(\mathbf{3}, 7, 5, \mathbf{1}) &= I_H(\mathbf{3}, 5, \mathbf{1}, \mathbf{1}), \\ I_A(\mathbf{3}, 7, 6, \mathbf{2}) &= I_H(\mathbf{3}, 5, \mathbf{1}, \mathbf{2}), \\ I_A(\mathbf{6}, 2, 3, 7) &= I_H(\mathbf{6}, 4, 8, 7), \\ I_A(\mathbf{6}, 2, 4, \mathbf{8}) &= I_H(\mathbf{6}, 4, 8, \mathbf{8}). \end{aligned}$$

These all follow from the classical relationship $(TS)^3 = \text{Id}$ on the generators of $\text{PSL}(2, \mathbb{Z})$. An equivalent formulation is $\tilde{S}\tilde{T}\tilde{S} = \tilde{T}^{-1}\tilde{S}\tilde{T}^{-1}$. By definition,

$$I_A(3, 7, 5, 1) = A_3^{-1}A_7^{-1}A_5^{-1}(I_1) = \tilde{S}\tilde{T}\tilde{S}(I_1)$$

and

$$I_H(3, 5, 1, 1) = H_3^{-1}H_5^{-1}H_1^{-1}(I_1) = \tilde{T}^{-1}\tilde{S}\tilde{T}^{-1}(I_1);$$

because $\tilde{S}\tilde{T}\tilde{S} = \tilde{T}^{-1}\tilde{S}\tilde{T}^{-1}$, we have $I_A(3, 7, 5, 1) = I_H(3, 5, 1, 1)$. The other three relations are proved similarly. Alternatively, this can be proved by tracking the image of I_1 under the relevant maps shown in figure 6.

Notice that the recoding relations do not affect the first and fourth digit. This means that the recoding process will be localized to these words of length 4, and it does not affect the symbols on either side of the block.

We refer to the four words

$$3751, \quad 3762, \quad 6237, \quad 6248$$

as ‘exceptional blocks’. Our goal is to prove lemma 7 by induction on the number ℓ of exceptional blocks that occur in ω .

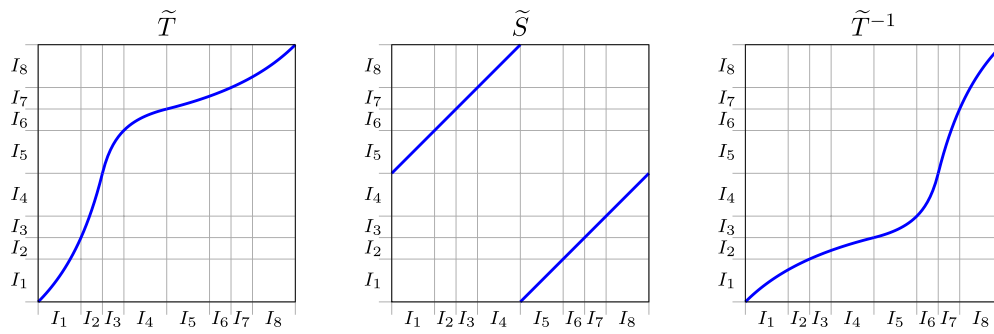


Figure 6. Graphs of \tilde{T} (left), \tilde{S} (middle), and \tilde{T}^{-1} (right), each with the Markov shared partition for Artin and Hurwitz maps.

Base case. If there are no exceptional blocks in $(\omega_0, \omega_1, \dots, \omega_n)$, then the sequence $(\omega_0, \omega_1, \dots, \omega_{n-2})$ will not contain the symbols 3 or 6 and so by the final statement of lemma 5 we have

$$\begin{aligned} I_A(\omega_0, \omega_1, \dots, \omega_n) &= A_{\omega_0}^{-1} \cdots A_{\omega_{n-2}}^{-1} (I_A(\omega_{n-1}, \omega_n)) \\ &= H_{\omega_0}^{-1} \cdots H_{\omega_{n-2}}^{-1} (I_H(\omega_{n-1}, \tau_n)) \\ &= I_H(\omega_0, \omega_1, \dots, \omega_{n-1}, \tau_n), \end{aligned}$$

where τ_n is determined from the matching $I_A(\omega_{n-1}, \omega_n) = I_H(\omega_{n-1}, \tau_n)$ (see figure 5).

Induction step. Now assume that the statement of lemma 7 is true for any A -admissible finite sequence ω that contains $\ell > 0$ exceptional blocks; we will prove that the statement holds for any word $(\omega_0, \omega_1, \dots, \omega_n)$ that contains $\ell + 1$ exceptional blocks.

Let k be the index where the first exceptional block appears. From the induction assumption,

$$I_A(\omega_{k+3}, \omega_{k+4}, \dots, \omega_n) = I_H(\tau_{k+3}, \tau_{k+4}, \dots, \tau_n),$$

where $\tau_{k+3} = \omega_{k+3}$; if $\omega_n \in \{1, 8\}$ then $\omega_n = \tau_n$. If $\omega_n = 2$ then $\tau_n \in \{2, 4\}$; and if $\omega_n = 7$ then $\tau_n \in \{5, 7\}$.

Now, finally, we have

$$\begin{aligned} I_A(\omega) &= I_A(\omega_0, \omega_1, \dots, \omega_{k-1}, \omega_k, \omega_{k+1}, \omega_{k+2}, \omega_{k+3}, \dots, \omega_n) \\ &= A_{\omega_0}^{-1} \cdots A_{\omega_{k-1}}^{-1} A_{\omega_k}^{-1} A_{\omega_{k+1}}^{-1} A_{\omega_{k+2}}^{-1} (I_A(\omega_{k+3}, \dots, \omega_n)) \\ &= H_{\omega_0}^{-1} \cdots H_{\omega_{k-1}}^{-1} H_{\omega_k}^{-1} H_{\tau_{k+1}}^{-1} H_{\tau_{k+2}}^{-1} (I_H(\omega_{k+3}, \dots, \tau_n)) \\ &= I_H(\omega_0, \omega_1, \dots, \omega_{k-1}, \omega_k, \tau_{k+1}, \tau_{k+2}, \omega_{k+3}, \dots, \tau_n) \\ &= I_H(\tau). \end{aligned}$$

□

With the recoding process (lemma 7) in place, we return to showing that $\psi_A = \psi_H$.

Proof of theorem 6. By the assumptions of lemma 7, it is enough to show that $\rho'_A(I_A(\omega)) = \rho'_H(I_A(\omega))$ for $\omega_n \in \{1, 2, 7, 8\}$. Fix $\omega = (\omega_0, \dots, \omega_n)$ and let $\tau = (\tau_0, \dots, \tau_n)$ be the corresponding H -admissible word from lemma 7.

Since ϕ_A maps the cylinder interval $I_A(\omega)$ exactly to the symbolic cylinder $C_A(\omega)$,

$$\rho'_A(I_A(\omega_0, \dots, \omega_n)) = \frac{v_{\omega_n}}{\lambda^n}.$$

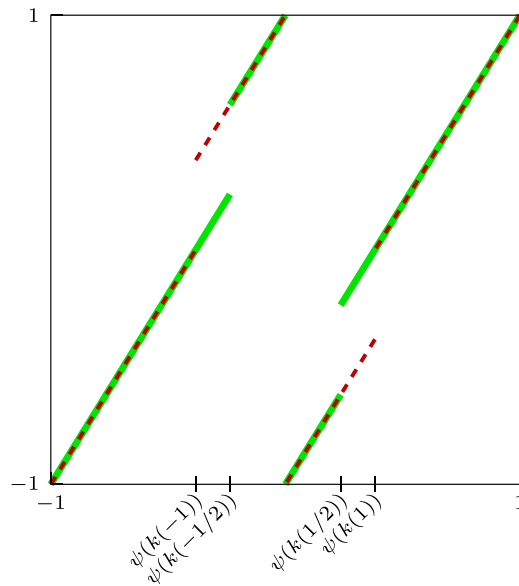


Figure 7. Partially-overlapping graphs of $\psi \circ \tilde{f}_A \circ \psi^{-1}$ (dashed) and $\psi \circ \tilde{f}_H \circ \psi^{-1}$ (solid).

Because $I_A(\omega_0, \dots, \omega_n) = I_H(\tau_0, \dots, \tau_n)$, and ϕ_H maps the cylinder interval $I_H(\tau)$ exactly to the symbolic cylinder $C_H(\tau)$, in fact

$$\rho'_H(I_A(\omega_0, \dots, \omega_n)) = \rho'_H(I_H(\tau_0, \dots, \tau_n)) = \frac{v_{\tau_n}}{\lambda^n}.$$

The claim $\rho'_A(I_A(\omega)) = \rho'_H(I_A(\omega))$ is now equivalent to $v_{\omega_n} = v_{\tau_n}$, and this is easily checked using (6) and the final parts of lemma 7. If $\omega_n \in \{1, 8\}$ then $\omega_n = \tau_n$ (so trivially $v_{\omega_n} = v_{\tau_n}$). If $\omega_n = 2$ then $\tau_n \in \{2, 4\}$, and since $v_2 = v_4$ this is also fine. Similarly, if $\omega_n = 7$ then $\tau_n \in \{5, 7\}$ is sufficient because $v_5 = v_7$.

Having proven that $\rho'_A(I_A(\omega)) = \rho'_H(I_A(\omega))$ for a generating set of intervals $I_A(\omega)$, and using the definition (4), we conclude that $\psi_A = \psi_H$. □

2.3. Proof of theorem 1

Since $\psi_A = \psi_H$ by theorem 6, we will now denote these two maps by simply ψ . The map \tilde{f}_H acts as \tilde{T} on the interval $k([-\infty, -\frac{1}{2}]) = [-1, -\frac{1}{3}]$, so by construction, $\psi \circ \tilde{T} \circ \psi^{-1}$ is linear (with slope $\lambda = \frac{1+\sqrt{5}}{2}$, which we now refrain from repeating) on the interval $\psi([-1, -\frac{1}{3}])$. Similarly, \tilde{f}_A acts as \tilde{S} on $k([-1, 1]) = [-\frac{1}{2}, \frac{1}{2}]$ and so $\psi \circ \tilde{S} \circ \psi^{-1}$ is linear on $\psi([- \frac{1}{2}, \frac{1}{2}])$. And because \tilde{f}_H acts as \tilde{T}^{-1} on $[\frac{1}{3}, 1]$, we know that $\psi \circ \tilde{T}^{-1} \circ \psi^{-1}$ is linear on $\psi([\frac{1}{3}, 1])$. See figure 7.

The map ψ therefore satisfies the following four conditions:

- (i) for $x \in \psi([-1, -\frac{1}{3}])$, $\psi(\tilde{T}(\psi^{-1}(x))) = \lambda x + c_1$;
- (ii) for $x \in \psi([- \frac{1}{2}, 0])$, $\psi(\tilde{S}(\psi^{-1}(x))) = \lambda x + c_2$;
- (iii) for $x \in \psi([0, \frac{1}{2}])$, $\psi(\tilde{S}(\psi^{-1}(x))) = \lambda x + c_3$;
- (iv) for $x \in \psi([\frac{1}{3}, 1])$, $\psi(\tilde{T}^{-1}(\psi^{-1}(x))) = \lambda x + c_4$.

In fact, one can calculate $c_1 = \lambda - 1, c_2 = 1, c_3 = -1, c_4 = 1 - \lambda$, but these are not necessary for the proof.

Let $(a, b) \in [-1, -\frac{1}{2}] \times [\frac{1}{2}, 1]$ be arbitrary. The map $\tilde{f}_{a,b}$ acts as \tilde{T} on the interval

$$[-1, k(a)] \subset [-1, -\frac{1}{3}],$$

and since $\psi \circ \tilde{T} \circ \psi^{-1}$ is linear on all of $\psi([-1, -\frac{1}{3}])$ by (i), we have that $\psi \circ \tilde{f}_{a,b} \circ \psi^{-1}$ is linear on $\psi([-1, k(a)]) \subset \psi([-1, -\frac{1}{3}])$.

Similarly, $\psi \circ \tilde{f}_{a,b} \circ \psi^{-1}$ is linear on $\psi([k(a), 0])$ because $\tilde{f}_{a,b}$ acts by \tilde{S} on $[k(a), 0] \subset [-\frac{1}{2}, 0]$ and, by (ii), $\psi \circ \tilde{S} \circ \psi^{-1}$ is linear on all of $\psi([-\frac{1}{2}, 0])$. Likewise, $\psi \circ \tilde{f}_{a,b} \circ \psi^{-1}$ is linear on $\psi([0, k(b)]) \subset \psi([0, \frac{1}{2}])$ by (iii) and on $\psi([k(b), 1]) \subset \psi([-\frac{1}{3}, 1])$ by (iv).

Since $\tilde{f}_{a,b}$ is conjugate to a map with constant slope λ on all of $[-1, 1]$, we have $h_{\text{top}}(\tilde{f}_{a,b}) = \log(\lambda) = \log(\frac{1+\sqrt{5}}{2})$ by [21]. □

3. Further remarks and open questions

3.1. Slow Gauss map

Let $g : [0, \infty] \rightarrow [0, \infty]$ be the classical ‘slow Gauss map’

$$g(x) = \begin{cases} 1/x & \text{if } 0 \leq x < 1 \\ x - 1 & \text{if } x \geq 1, \end{cases}$$

which is closely related with a regular (plus) continued fraction expansion: for $0 < x < 1$,

$$x = \frac{1}{n_1 + \frac{1}{n_2 + \frac{1}{n_3 + \dots}}} := [0, n_1, n_2, n_3, \dots]$$

where the digits n_k are the number of consecutive iterates under g that are in $[1, \infty]$ between visits to $[0, 1)$. Let $\tilde{g} : [0, 1] \rightarrow [0, 1]$ be the compactified version, $\tilde{g} = k \circ g \circ k^{-1}$, where $k : [0, \infty] \rightarrow [0, 1]$ is $k(x) = \frac{x}{1+x}$. In [8], Bowen considered measure-theoretic properties of these two maps.

The map $\tilde{g} : [0, 1] \rightarrow [0, 1]$ is semi-conjugate to $\tilde{f}_{-1,1} : [-1, 1] \rightarrow [-1, 1]$ via the absolute value function $\text{abs} : [-1, 1] \rightarrow [0, 1]$, that is $g \circ \text{abs} = \text{abs} \circ \tilde{f}_{-1,1}$, so g is a topological factor of $\tilde{f}_{-1,1}$. Although in general the topological entropy of a factor is only less than or equal to the topological entropy of the map, in this case we have equality of topological entropies: the map \tilde{g} has the Markov partition $\{I_1, I_2\} = \{[0, \frac{1}{2}], [\frac{1}{2}, 1]\}$ with transition matrix $\begin{pmatrix} 0 & 1 \\ 1 & 1 \end{pmatrix}$, which immediately gives that $h_{\text{top}}(\tilde{g}) = \log(\frac{1+\sqrt{5}}{2})$. The reason for the equality is a simple relationship between the regular continued fraction expansion and a $(-1, 1)$ -continued fraction expansions: for $0 < x \leq 1$,

$$x = [0, n_1, n_2, \dots] = [0, -n_1, n_2, -n_3, \dots]_{-1,1}.$$

3.2. Conjectures about entropy

Outside of the square $\mathcal{S} = [-1, -\frac{1}{2}] \times [\frac{1}{2}, 1]$, there are many unanswered questions about the behavior of $h_{\text{top}}(f_{a,b})$. Using Markov partitions, we can calculate explicit entropy values for many rational values (a, b) , and from these we have created figure 8.

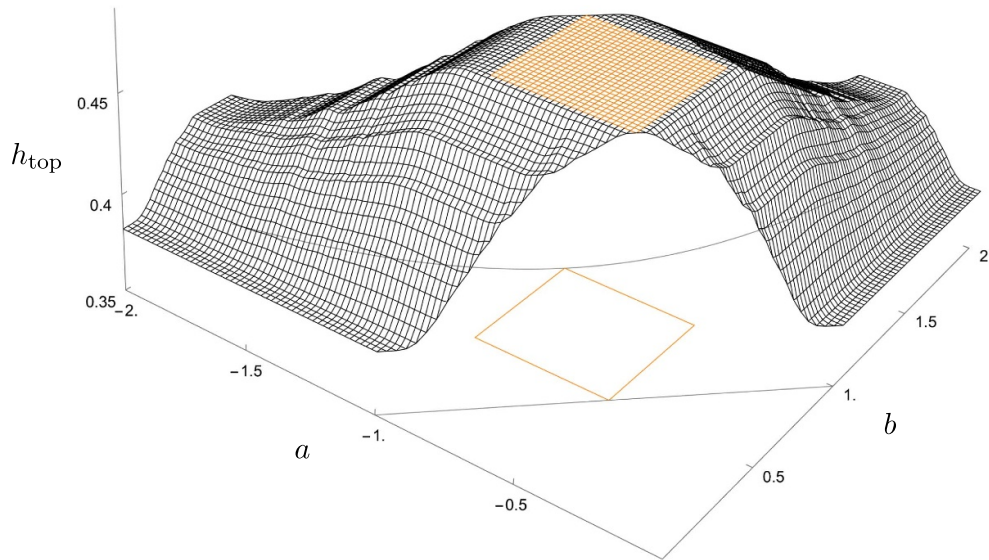


Figure 8. Numerical plot of topological entropy (plateau is $(a, b) \in \mathcal{S}$).

While in section 2 we focused on the parameter choices $(-1, 1)$ and $(-\frac{1}{2}, \frac{1}{2})$, the map for the case $(a, b) = (-1, 0)$ has also been studied independently, as it corresponds to classical backwards continued fractions [2, 15]. Additionally, according to our numerical tests, this parameter appears to give the minimum possible value for $h_{top}(f_{a,b})$.

We can directly calculate the value

$$h_{top}(f_{-1,0}) = \log(\kappa) \approx 0.382,$$

where κ is the spectral radius of

$$M_{-1,0} = \begin{pmatrix} 1 & 1 & 0 & 0 \\ 0 & 0 & 0 & 1 \\ 0 & 1 & 0 & 0 \\ 0 & 0 & 1 & 1 \end{pmatrix}$$

and satisfies $\kappa^3 - \kappa^2 - 1 = 0$.

Conjecture 1 (Flexibility).

- (i) If $(a, b) \in \mathcal{P}$ then $\log(\kappa) \leq h_{top}(f_{a,b}) \leq \log(\frac{1+\sqrt{5}}{2})$.
- (ii) For any $h \in [\log(\kappa), \log(\frac{1+\sqrt{5}}{2})]$, there exists $(a, b) \in \mathcal{P}$ with $h_{top}(f_{a,b}) = h$.

Conjecture 2 (Continuity and monotonicity).

- (i) The function $(a, b) \mapsto h_{top}(f_{a,b})$ is continuous.
- (ii) For fixed $b \leq \frac{1}{2}$, the function $a \mapsto h_{top}(f_{a,b})$ is monotone non-decreasing.

There are some line segments in figure 8 but outside of \mathcal{S} that appear to be horizontal, a phenomenon noticed in [6, 9] for some one-parameter families of maps. In figure 9 this is much

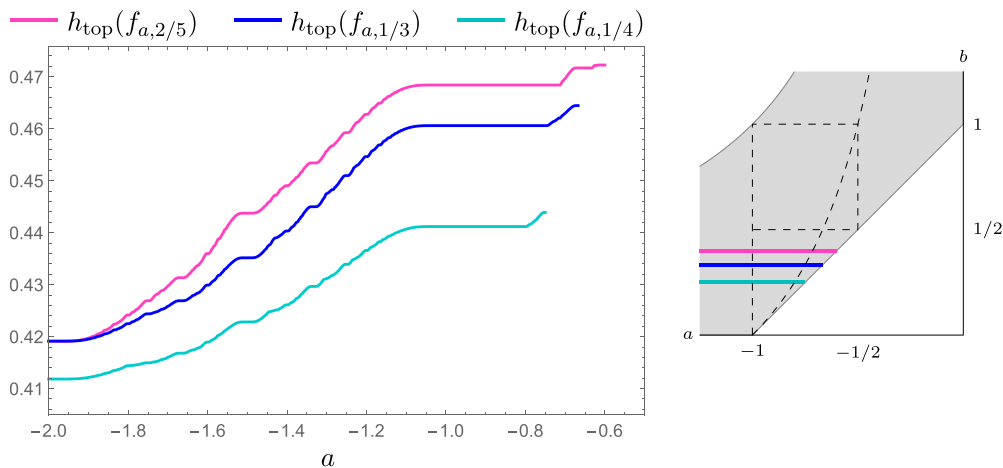


Figure 9. Plots of entropy for some fixed values of b .

clearer: each curve has a flat section toward the right. For each value of b , the flat section of the curve occurs for $a \in [-1, -\frac{1}{b+1}]$, so this is described explicitly in conjecture 3.

Conjecture 3. *If $b \leq \frac{1}{2}$ and $-1 \leq a \leq -\frac{1}{b+1}$ then $h_{\text{top}}(f_{a,b}) = h_{\text{top}}(f_{-1,b})$. That is, $h_{\text{top}}(f_{a,b})$ is independent of a in the region $\{(a,b) \in \mathcal{P} \mid b \leq \frac{1}{2}, -1 \leq a \leq -\frac{1}{b+1}\}$.*

One method to prove conjecture 3 would be to prove that $\psi_{-1,b} = \psi_{-1/(b+1),b}$ for each $b \in [0, 1]$. For some individual (rational) values of b , the authors have found a recoding from $(-1, b)$ to $(-\frac{1}{b+1}, b)$, similar to the recoding from $(-1, 1)$ to $(-\frac{1}{2}, \frac{1}{2})$ presented in section 2.2. However, it is not clear how to generalize those recodings to other $b \in [0, \frac{1}{2}]$.

Although $f_{-1,1}$ (Artin) and $f_{-1,0}$ are well-studied, we do not have any explicit formula for $h_{\text{top}}(f_{-1,b})$ in general; numerically calculated values are shown in figure 10. This figure also shows entropy of $f_{b-1,b}$, the one-parameter family along the boundary of \mathcal{P} that is conceptually similar to the so-called Japanese continued fractions. Note that the two curves in figure 10 intersect *only* at $(0, \log(\kappa))$ and $(\frac{1}{2}, \log(\frac{1+\sqrt{5}}{2}))$; for all $0 < b < \frac{1}{2}$ we have (numerically) that $h_{\text{top}}(f_{b-1,b}) > h_{\text{top}}(f_{-1,b})$. Theorem 1 implies that the right half of the $h_{\text{top}}(f_{-1,b})$ curve is flat because $a = -1, b > \frac{1}{2}$ is an edge of the golden square. Also, the symmetry of the $h_{\text{top}}(f_{b-1,b})$ curve is because $f_{a,b}$ and $f_{-b,-a}$ are conjugate.

3.3. Cycle property (matching) and entropy plateau

In 2019, Bruin, Carminati, Marmi, and Profeti [9] proved that entropy plateau for a one-parameter family of affine maps of an interval with a single point of discontinuity occurs when the two orbits of the discontinuity point *match* after the same number of iterations (a property called *neutral matching*). Already in 2010 the authors in [17] proved that the *matching* for (a,b) -continued fractions occurs for essentially all $(a,b) \in \mathcal{P}$ (they called it *the cycle property*): specifically, the parameter a has the cycle property if there exist nonnegative integers m_a and k_a such that

$$f_{a,b}^{m_a}(Sa) = f_{a,b}^{k_a}(Ta),$$

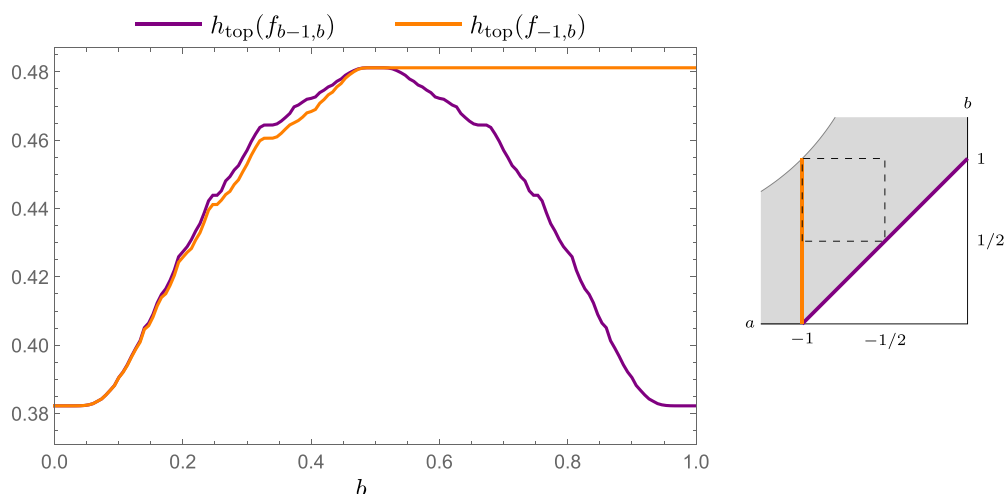


Figure 10. Plots of entropy for one-parameter families.

and, similarly, b has the cycle property if there exist nonnegative integers m_b and k_b such that

$$f_{a,b}^{m_b}(T^{-1}b) = f_{a,b}^{k_b}(Sb).$$

In [19] they proved the cycle property for boundary maps associated to Fuchsian groups, another example of piecewise continuous piecewise monotone maps of the circle. In the (a, b) -case, the upper and lower cycles may be of arbitrary length while in the Fuchsian case the cycles are always the same length. In the Fuchsian case we proved ‘entropy rigidity’, that is, the entropy is constant on the entire parameter space [1]. In the (a, b) -case, we proved entropy plateau in the golden square \mathcal{S} . In fact, generic $(a, b) \in \mathcal{S}$ has neutral matching (i.e. $m_a = k_a$ and $m_b = k_b$), although the lengths can be arbitrary large (this can be proved by carefully following the analysis of [17, sections 4 and 8]).

It *might* be possible to prove that h_{top} is constant in the golden square directly from the neutral matching property. Such a proof would be in the spirit of Bruin *et al* [9]. In the co-compact Fuchsian setting of [1, 19] the cycles are always the same length, so this argument, if possible, would provide alternative proofs of [1, theorem 1] and this paper’s theorem 1 together.

Data availability statement

All data that support the findings of this study are included within the article (and any supplementary files).

ORCID iDs

Adam Abrams  <https://orcid.org/0000-0001-6883-2661>
 Ilie Ugarcovici  <https://orcid.org/0000-0003-4548-9519>

References

- [1] Abrams A, Katok S and Ugarcovici I 2023 Rigidity of topological entropy of boundary maps associated to Fuchsian groups *A Vision for Dynamics in the 21st Century* (Cambridge: Cambridge University Press)
- [2] Adler R and Flatto L 1984 The backward continued fraction map and geodesic flow *Ergod. Theory Dyn. Syst.* **4** 487–92
- [3] Adler R, Konheim A and McAndrew M 1965 Topological entropy *Trans. Amer. Math. Soc.* **114** 309–19
- [4] Alsedà L, Llibre J and Misiurewicz M 2000 *Combinatorial Dynamics and Entropy in Dimension One (Advanced Series in Nonlinear Dynamics vol 5)*, 2nd edn (River Edge, NJ: World Scientific Publishing Co. Inc)
- [5] Alsedà L and Misiurewicz M 2015 Semiconjugacy to a map of a constant slope *Discrete Continuous Dyn. Syst. B* **20** 3403–13
- [6] Botella-Soler V, Oteo J A, Ros J and Glendinning P 2013 Lyapunov exponent and topological entropy plateaus in piecewise linear maps *J. Phys. A* **46** 26
- [7] Bowen R 1971 Entropy for group endomorphisms and homogeneous spaces *Trans. Amer. Math. Soc.* **153** 401–14 Bowen R 1973 *Trans. Amer. Math. Soc.* 181 509–10 (erratum)
- [8] Bowen R 1979 Invariant measures for Markov maps of the interval *Commun. Math. Phys.* **69** 1–17
- [9] Bruin H, Carminati C, Marmi S and Profeti A 2019 Matching in a family of piecewise affine maps *Nonlinearity* **32** 172–208
- [10] Cospè D and Misiurewicz M 2018 Entropy locking *Fundam. Math.* **241** 83–96
- [11] de Melo W and van Strien S 1993 *One-Dimensional Dynamics* Ergebnisse der Mathematik und Ihrer Grenzgebiete (Berlin: Springer)
- [12] Dinaburg E 1970 The relation between topological entropy and metric entropy *Soviet Math. Dokl.* **11** 13–16
- [13] Kameyama A 2002 Topological transitivity and strong transitivity *Acta Math. Univ. Comenianae* **2** 139–45
- [14] Katok A and Hasselblatt B 1995 *Introduction to the Modern Theory of Dynamical Systems* Encyclopedia of Mathematics and its Applications (Cambridge: Cambridge University Press)
- [15] Katok S 1996 Coding of closed geodesics after Gauss and Morse *Geom. Dedicata* **63** 123–45
- [16] Katok S and Ugarcovici I 2005 Arithmetic coding of geodesics on the modular surface via continued fractions *CWI Tract.* **135** 59–77
- [17] Katok S and Ugarcovici I 2010 Structure of attractors for (a, b) -continued fraction transformations *J. Mod. Dyn.* **4** 637–91
- [18] Katok S and Ugarcovici I 2012 Applications of (a, b) -continued fraction transformations *Ergod. Theory Dyn. Syst.* **32** 755–77
- [19] Katok S and Ugarcovici I 2017 Structure of attractors for boundary maps associated to Fuchsian groups *Geom. Dedicata* **191** 171–98
- [20] Krengel U 1967 Entropy of conservative transformations *Z. Wahrscheinlichkeitstheor. Verwandte Geb.* **7** 161–81
- [21] Misiurewicz M and Szlenk W 1980 Entropy of piecewise monotone mappings *Stud. Math.* **67** 45–63
- [22] Misiurewicz M and Ziemian K 1992 Horseshoes and entropy for piecewise continuous piecewise monotone maps *From Phase Transitions to Chaos* (River Edge, NJ: World Scientific) pp 489–500
- [23] Parry W 1964 Intrinsic Markov chains *Trans. Amer. Math. Soc.* **112** 55
- [24] Parry W 1966 Symbolic dynamics and transformations of the unit interval *Trans. Amer. Math. Soc.* **122** 368–78